Electrokinetic Focusing Injection Methods on Microfluidic Devices

ARTICLE *in* ANALYTICAL CHEMISTRY · MAY 2003

Impact Factor: 5.64 · DOI: 10.1021/ac020741d · Source: PubMed

3 AUTHORS:

Lung-Ming Fu
National Pingtung University of Science and …
134 PUBLICATIONS **2,503** CITATIONS
SEE PROFILE

Ruey-Jen Yang
National Cheng Kung University
164 PUBLICATIONS **2,753** CITATIONS
SEE PROFILE

Gwo-Bin Lee
National Tsing Hua University
422 PUBLICATIONS **7,341** CITATIONS
SEE PROFILE

Anal. Chem. **2003,** *75,* 1905−1910

Electrokinetic Focusing Injection Methods on Microfluidic Devices

Lung-Ming Fu, Ruey-Jen Yang, and Gwo-Bin Lee*

Department of Engineering Science, National Cheng Kung University, Tainan, 70101 Taiwan

This paper presents an experimental and numerical investigation into electrokinetic focusing injection on microfluidic chips. The valving characteristics on microfluidic devices are controlled through appropriate manipulations of the electric potential strengths during the sample loading and dispensing steps. The present study also addresses the design and testing of various injection systems used to deliver a sample plug. A novel double-cross injection microfluidic chip is fabricated, which employs electrokinetic focusing to deliver sample plugs of variable volume. The proposed design combines several functions of traditional sample plug injection systems on a single microfluidic chip. The injection technique uses an unique sequence of loading steps with different electric potential distributions and magnitudes within the various channels to effectuate a virtual valve.

Microfluidic devices have been used successfully in a variety of separation techniques associated with the performance of chemical or biological assays, e.g., the separation of DNA for genetic engineering purposes. Microchip-based separation techniques are essential elements in the development of micro total analysis systems (μ-TAS). A comprehensive overview of the μ-TAS devices in theory, technology, and analytical operations as well as applications was given in refs 1 and 2. Among them, microchip capillary electrophoresis (CE)[3−8] has been utilized as the principal analytical technique for these μ-TAS devices. The underpinning principle of all these techniques is the ability to control the mobility of differently charged particles by the appropriate application of an external electric field. Such chips often use electrokinetic manipulation techniques to handle and analyze the fluid, and by coupling the chip with other analytical techniques such as mass spectroscopy, it is possible to provide a complete chemical analysis system that satisfies the lab-on-a-chip concept, e.g., PCR-CE,[9−11] CE-multifraction collection,[12] DEP−CE (DNA collection and separation),[13] and CE-optical waveguides.[14]

The injection system on a microfluidic chip is one of the key elements in the sample-handling process, and its characteristics determine the quality of the separation achieved. Therefore, a thorough understanding of the mechanisms that govern electrokinetic manipulations, particularly those associated with discrete injections, is essential if the microfluidic chip design is to be optimized. A review of the published literature reveals many studies concerning injection methods implemented on microfluidic chips. For example, the sample valves required to deliver discrete injections have been developed by using various electrokinetic methods, e.g., the T-form,[15] cross-form,[16−20] and double-T-form[21−23] injection methods. Generally, these injection systems are only capable of delivering a fixed-volume sample plug into the separation channel. However, some detection cases require the delivery of variable-volume plugs. Clearly, in these cases, a fixed-volume injection system is inappropriate. The current authors have previously investigated various variable-volume injection methods, including the multi-T-form[24] and the double-cross-form.[25] The present study uses theoretical and experimental approaches to

* Corresponding author. E-mail: gwobin@mail.ncku.edu.tw. Tel: +886-6-275-7575 Ext. 63347. Fax: +886-6-276-1687.

(1) Reyes, D. R.; Iossifidis, D.; Auroux, P.-A.; Manz, A. *Anal. Chem.* **2002**, *74*, 2623−2636.
(2) Auroux, P.-A.; Iossifidis, D.; Reyes, D. R.; Manz, A. *Anal. Chem.* **2002**, *74*, 2637−2652.
(3) Khandurina, J.; Jacobson, S. C.; Waters, L. C.; Foote, R. S.; Ramsey, J. M. *Anal. Chem.* **1999**, *71*, 1815−1819.
(4) Culbertson, C. T.; Ramsey, R.; Ramsey, J. M. *Anal. Chem.* **2000**, *72*, 2285−2291.
(5) Gottschlich, N.; Jacobson, S. C.; Culbertson, C. T.; Ramsey, J. M. *Anal. Chem.* **2001**, *73*, 2669−2674.
(6) Heller, C. *Electrophoresis* **2001**, *22*, 629−643.
(7) Rochu, D.; Masson, P. *Electrophoresis* **2002**, *23*, 189−202.
(8) Mistry, K.; Krull, I.; Grinberg, N. *J. Sep. Sci.* **2002**, *25*, 935−958.
(9) Woolley, A. T.; Hadley, D.; Landre, P.; deMello, A. J.; Mathies, R. A.; Northrup, M. A. *Anal. Chem.* **1996**, *68*, 4081−4086.
(10) Khandurina, J.; McKnight, T. E.; Jacobson, S. C.; Waters, L. C.; Foote, R. S.; Ramsey, J. M. *Anal. Chem.* **2000**, *72*, 2995−3000.
(11) Verpoorte, E. *Electrophoresis* **2002**, *23*, 677−712.
(12) Khandurina, J.; Chovan, T.; Guttman, A. *Anal. Chem.* **2002**, *74*, 1737−1740.
(13) Cui, L.; Holmes, D.; Morgan, H. *Electrophoresis* **2001**, *22*, 3893−3901.
(14) Lin, C. H.; Lee, G. B.; Lin, C. C.; Chen, S. H.; Chang, G.. L. *Micro-TAS 2002*, Nara, Japan, November 3−7, 2002; pp 730∼732.
(15) Harrison, D. J.; Manz, A.; Fan, Z.; Ludi, H.; Widmer, H. M. *Anal. Chem.* **1992**, *64*, 1926−1932.
(16) Jacobson, S. C.; Culbertson, C. T.; Daler, J. E.; Ramsey, J. M. *Anal. Chem.* **1998**, *70*, 3476−3480.
(17) Ermakov, S. V.; Jacobson, S. C.; Ramsey, J. M. *Anal. Chem.* **2000**, *72*, 3512−3517.
(18) Alarie, J. P.; Jacobson, S, C.; Culbertson, C. T.; Ramsey, J. M. *Electrophoresis* **2000**, *21*, 100−106.
(19) Crabtree, H. J.; Cheong, E. C. S.; Tilroe, D. A.; Backhouse, C. J. *Anal. Chem.* **2001**, *73*, 4079−4086.
(20) Alarie, J. P.; Jacobson, S, C.; Ramsey, J. M. *Eletrophoresis* **2001**, *22*, 312−317.
(21) Effenhauser, C. S.; Maze, A.; Widmer, H. M. *Anal. Chem.* **1993**, *65*, 2673−2642.
(22) Koutny, L. B.; Schmalzing, D.; Taylor, T. A.; Fuchs, M. *Anal. Chem.* **1996**, *68*, 18−22.
(23) Ocvirk, G.; Munroe, M.; Tang, T.; Oleschuk, R.; Westra, K.; Harrison, D. J. *Electrophoresis* **2000**, *21*, 107−115.
(24) Fu, L.-M.; Yang, R.-J.; Lee, G.-B.; Liu, H.-H. *Anal. Chem.* **2002**, *74*, 5084−5091.
(25) Fu, L.-M.; Yang, R.-J.; Lee, G.-B. *J, Sep. Sci.* **2002**, *25*, 996−1010.

10.1021/ac020741d CCC: $25.00
Published on Web 03/14/2003

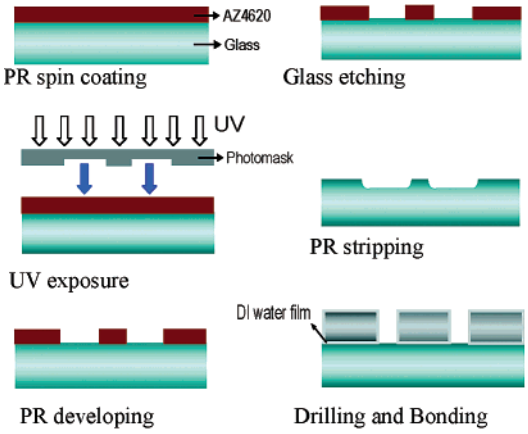

Figure 1. Fabrication of glass-based microchannel.

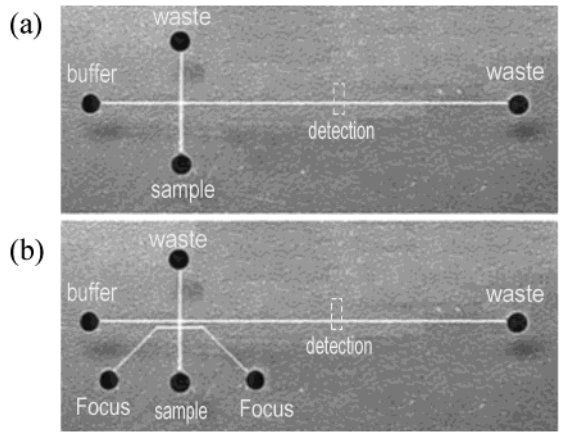

Figure 2. Photograph of two injection systems: (a) cross and (b) double-cross.

investigate the use of electrokinetic focusing to control the volume of the sample plug delivered into the separation channel and introduces the design of a novel double-cross injection system, which overcomes the limitations of the fixed-volume injection systems.

The aim of this study is to design a multifunction injection system on a microfluidic chip. The parameters that are key in controlling the shape of the injection sample plug are determined through model simulations, and the effects of operating parameters such as electric potential and flow field are studied. The optimum design of the injection channels is established, and the ideal operating conditions are investigated. Finally, the theoretical results are used to fabricate and test several injection microfluidic chips.

EXPERIMENTAL SECTION

Microfabrication. In this study, commercially available microscope glass slides of dimensions 76 × 26 × 1 mm^3 have been used, supplied by Marienfeld. Prior to microfabrication of the glass chips, the slides were first annealed at 400 °C for 4 h in order to relieve their internal residual stress. The photomasks were generated using layout software (AutoCAD) and were printed (10 000 dpi). Figure 1 illustrates the microfabrication process[26] used in this study. Initially, the glass slide was cleaned with a piranha solution (H_2SO_4 (%):H_2O_2 (%) = 3:1) for 10 min. It was then rinsed in deionized (DI) water and blown dry with nitrogen gas. To ensure the complete removal of residual water molecules, a dehydration process was carried out by baking the slides on a hot plate for 3 min at a temperature of 100 °C.

Following the dehydration process, the slide was coated with the AZ4620 positive photoresist (PR) using a spin coater and then baked at 100 °C for a further 3 min. After soft baking, the thickness of the PR layer was measured to be ~3 μm. The UV lithography was processed using a mask aligner (OAI Corp.) with an exposure dose of 180 mJ·cm^{-2} for 12 s. Development of the PR was accomplished in 70 s by immersing the exposed substrate into a developer solution (AZ400k:DI water = 1:3). The resulting photoresist patterns were then hard-baked at 150 °C for 10 min. The baked PR layer is able to accommodate BOE (6:1) etching for as long as 40 min. In the process, to remove precipitated particles, the etching process was interrupted every 5 min and the substrates were dipped in a 1 M HCl solution for 10 s during the etching process. After the HCl dripping, the substrates were then cleaned by dripping in DI water and then immersing into the BOE etchant again. The etching and deprecipitation process were repeated until the etching process was finished.

Through holes with a diameter of 1.5 mm were drilled for sample inlets and outlets on another cover plate. The base and cover plates were fusion-bonded in a furnace at 580 °C for 20 min. The etching depth is 29.95 μm, and the surface roughness could be as small of 30 Å. Alternatively, a low-temperature glass bonding process using diluted HF (1%) has also been developed for sealing of microfluidic structures. Figure 2 shows the geometry of the injection microchannel on glass substrates after the photolithography process.

Detection. Performance of the microchips was monitored by a laser-induced fluorescence method using a charge-coupled device (CCD; model TE/CCD512TKM; Roper Scientific, Princeton, NJ) for imaging. An argon laser beam (514 nm) was used to induce fluorescent signals. The fluorescence was collected through a 50× microscope objective (Nikon, LU Plane), filtered spectrally (550 nm, cut-on), and measured by CCD. Rhodamine B (10^{-4} M) and Cy3 (6.5×10^{-3} M) were used as the test sample. The buffer used for experiments was 10 mM sodium borate (pH 9.2, Aldrich).

RESULTS AND DISCUSSION

The traditional design of the injection channel is in the form of a cross. A limitation of this configuration is that it is only able to inject discrete, fixed-volume samples. However, in certain instances, it may be necessary to provide different volumes of the sample to the detection and separation processes. The current study satisfies this requirement by developing a microfluidic device that features a double-cross injection microchannel configuration and that employs an electrokinetic focusing technique.

Although most previous studies regarding eletroosmotic flows[27−29] assumed the velocity profile to be fully developed in the microchannels, and considered the charge density to conform to the Boltzmann equilibrium distribution, these assumptions are

(26) Lin, C. H.; Lee, G. B.; Lin, Y. H.; Chang, G. L. *J. Micromech. Microeng.* **2001**, *11*, 726−732.
(27) Patankar, N. A.; Hu, H. H. *Anal. Chem.* **1998**, *70*, 1870−1881.
(28) Griffiths, S.; Nilson R. H. *Anal. Chem.* **2001**, *73*, 272−278.
(29) Erickson, D.; Li, D. *Langmuir* **2002**, *18*, 1883−1892.

not strictly valid since electroosmotic flow involves an entrance region within which neither condition is satisfied. To take account of this entrance effect, the current authors had previously developed physical models based on (a) the Poisson equation (ψ) for the electric potential and ζ potential for the fluid−solid boundary, (b) the Nernst_Planck equations (n^+, n^-) for the positive and negative ionic concentration, and (c) the full Navier−Stokes equations (u, v) modified to include the effects of the body force due to the electric and the charge density. The detailed expressions of the governing equation, the initial conditions, and the boundary conditions are provided in refs 30−32.

To predict the sample plug distribution in the separation channel, the equation for the diffusion of the sample will be solved by numerical simulation. We can obtain the sample plug distribution by solving the following nondimensional diffusion equation

$$\frac{\partial C}{\partial t} + u\cdot\nabla C = \frac{1}{Sc\{Re\}}\nabla^2 C \qquad (1)$$

where C is the sample concentration, Re is the Reynolds numbers, and Sc is the Schmidt number. For the flow conditions considered in the current investigation, the value of Sc in the equation given above is of the order of 10^5, while Re is of the order of 1. Although this implies that the diffusion term is very small in comparison to the convection term, diffusion is one of the primary mechanisms for sample dispersion, and accordingly, the term is retained in the numerical simulation. Since the sample concentration is carried passively by the flow field, eq 1 can be solved separately once the flow field has been determined.

In the current study, it is assumed that the microchannel is made of silica glass and that the buffer fluid is sodium borate. The physical and electrical properties of the liquid are as follows: dielectric constant $\epsilon = 80$, ζ potential of the channel wall −75 mV, applied electric field 0.1−1 kV/cm, electrokinetic diameter $\kappa = 32$, fluid viscosity $\mu = 10^{-3}$ N (s/m^2), Schmidt number of the charge density $Sc = 10^5$, and diffusion coefficient of the sample (hemoglobin) $D = 6.9 \times 10^{-11}$ m^2/s.

Electrokinetic Focusing Using a Single Cross-Injection System. As discussed above, the configuration most commonly adopted for the separation microchannels of microfluidic devices has always been the cross form presented in Figure 2a. The limitation of the traditional configuration (i.e., the volume of the delivered sample plug is fixed) may be overcome to a certain extent by focusing the electric field in the loading step. The appropriate controlling electric potential strength values during the loading and dispensing steps are provided in ref 25, together with a specification of suitable focusing ratios in the loading steps. Note that the focusing ratio is defined in terms of a scaling factor applied to the magnitude of the electric potential of the loading step. Table 1 presents the results for the four different focusing ratios considered in the current study, i.e., 1.0, 1.4, 1.8, and 2.2. Panels a and b of Figure 3 compare the sample stream distribution results obtained experimentally from CCD images with those predicted by numerical simulation for the four different focusing

Table 1

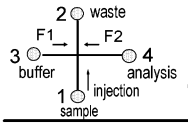	Electric potential strengths (kV)				
	ϕ_1	ϕ_2	ϕ_3=F$_1$	ϕ_4=F$_2$	Focusing ratio (F/$\phi_{3,case(a)}$)
Loading					
Case (a)	1	0	0.5	0.5	0.5/0.5=1
Case (b)	1	0	0.7	0.7	0.7/0.5=1.4
Case (c)	1	0	0.9	0.9	0.9/0.5=1.8
Case (d)	1	0	1.1	1.1	1.1/0.5=2.2
Dispensing	0.6	0.6	1.2	0	
Channel width (μm)	80				

strengths. A more quantitative comparison is presented in Figure 3c, which plots the concentration profiles at the sample waste channel cross section. Note that, in this figure, the experimental images obtained by mercury lamp-induced fluorescence are given in arbitrary units and the values are normalized. Meanwhile, the gray scale in the numerical simulation images represents the concentration distribution normalized relative to the initial (maximum) sample concentration. It can be seen that there is good qualitative agreement between the experimental results and those predicted numerically.

Panels a and b of Figure 4 show the shape of the sample plug in the separation channel of the single-cross injection system for a focusing ratio of 1.4 as predicted by the numerical simulation and as given by the experimental method, respectively. It is noted that the sample plug is rather slanted and that it has a conical shape, thus rendering it unsuitable for detection purposes.

Electrokinetic Focusing Using a Novel Double-Cross Injection System. It has been shown above that applying the electrokinetic focusing technique to the cross injection system distorts the shape of the sample plug in the separation channel and thus has a negative impact upon the quality of the separation. The current study develops a novel double-cross injection system on a single microfluidic chip and specifies the appropriate electrokinetic focusing required to deliver a suitable sample plug to the separation channel. The proposed double-cross injection system is presented in Figure 2b.

To investigate the influence of the focusing ratio, the sample distribution was determined experimentally and numerically for three different values of the ratio; i.e., $F/\phi = 1$, $F/\phi = 1.4$, and $F/\phi = 1.8$. Table 2 presents the corresponding results.

Figure 5 considers the case of a focusing ratio $F/\phi = 1$ and compares the sample distribution results determined by the experimental method with those predicted by the numerical simulation for the loading and dispensing steps in the double-cross injection system. When the electric field is activated for the loading step, the sample flows from channel 1 to the waste channel, 2. Simultaneously, an appropriate electric potential is applied to the buffer channel, 5, separation channel, 6, and focusing channels, 3 and 4, to prevent sample leakage. From Figure 5a, it can be seen that channels 3 and 4 are the major

(30) Yang, R.-J.; Fu, L.-M.; Hwang, C.-C. *J. Colloid Interface Sci.* **2001**, *244*, 173−179.
(31) Fu, L.-M.; Yang, R.-J.; Lee, G.-B. *Electrophoresis* **2002**, *23*, 602−612.
(32) Lin, J.-Y.; Fu, L.-M.; Yang, R.-J. *J. Micromech. Microeng.* **2002**, *12*, 955−961.

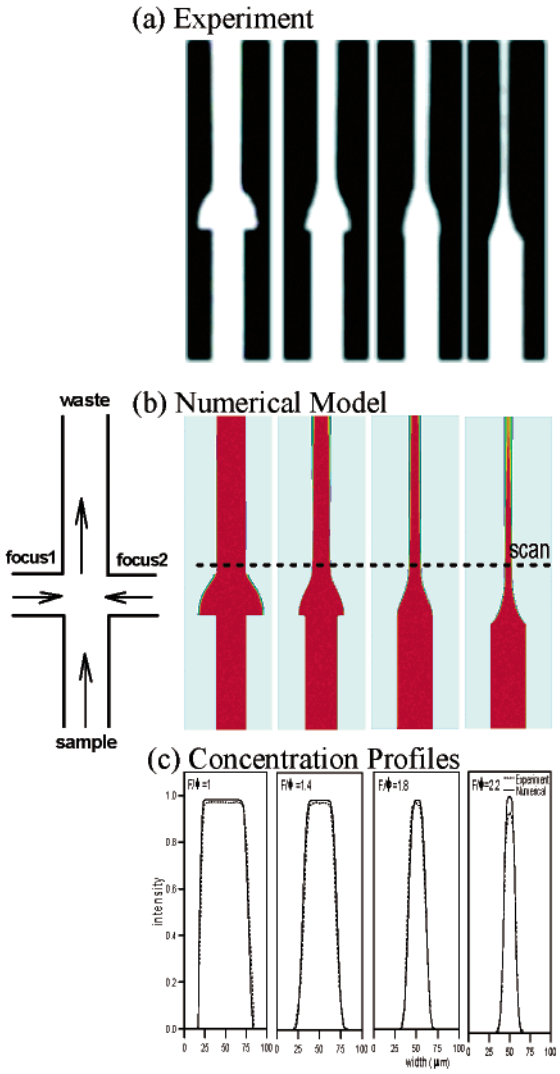

Figure 3. Comparison of the sample stream distribution results for the (a) experimental method, (b) the numerical simulation, and (c) concentration profiles across the scan area for different focusing ratios; i.e., $F/\phi = 1$, $F/\phi = 1.4$, $F/\phi = 1.8$, and $F/\phi = 2.2$, respectively.

focusing channels during the loading step and that channels 5 and 6 are the minor focusing channels. When the sample has filled the intersections between the separation channels (i.e., 5 and 6) and the injection channels (i.e., 1 and 2), the electric field switches immediately to the dispensing step. The sample in the intersection is forced to move into the separation channel, 6. Meanwhile, the sample in channels 1 and 2 is kept motionless in order to prevent sample leakage (Figure 5b). Although this injection mode closely resembles the traditional cross injection mode, the quality of the sample plug distribution in the separation channel is much improved.

Figure 6 plots the distribution of a sample injection for the double-cross injection system when a focusing ratio $F/\phi = 1.4$ is applied. In the loading step, the sample flows from channel 1 to the waste channel, 2. As shown in Figure 6a, the width of the sample concentration distribution in the downstream channel region is reduced for this particular value of the focusing ratio. The dispensing step procedure is exactly the same as in the previous case. However, the volume of the sample plug in the separation channel, 6, is seen to be smaller. Analysis of the

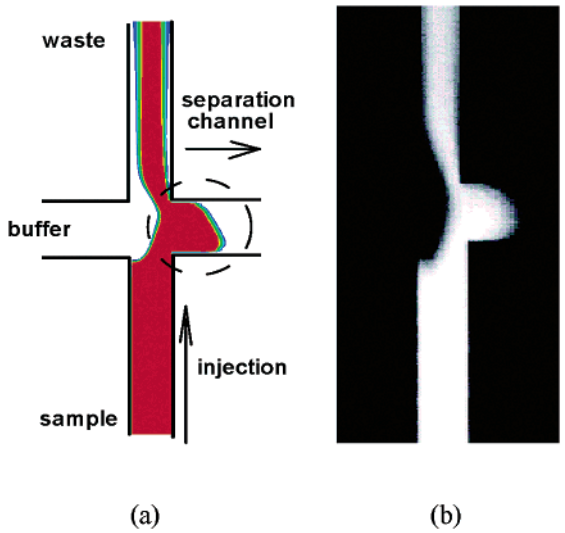

Figure 4. Comparison of the shape of the sample plug in the separation channel of the cross injection system using electrokinetic focusing with a focusing ratio of $F/\phi = 1.4$ for (a) the numerical model and (b) the experimental method.

Table 2

Electric potential strengths (kV)							
	ϕ_1	ϕ_2	$\phi_3=F_1$	$\phi_4=F_2$	ϕ_5	ϕ_6	Focusing ratio ($F/\phi_{3,\text{case(a)}}$)
Loading							
Case (a)	1	0	0.7	0.7	0.36	0.36	1
Case (b)	1	0	0.98	0.98	0.45	0.45	1.4
Case (c)	1	0	1.26	1.26	0.55	0.55	1.8
Dispensing	0.5	0.5	0.5	0.5	1	0	

Channel width = 80 (μm), H = 100 (μm)

experimental and the numerical results, respectively, shows that the plug volume is reduced to approximately 0.78 and 0.761 of the volume of the plug achieved with a focusing ratio of $F/\phi = 1$.

Figure 7 plots the distribution of a sample injection for the double-cross injection system using a focusing ratio of $F/\phi = 1.8$. The sample flows from channel 1 to channel 2 during the loading step. Meanwhile the buffer liquid in the focusing channels, 3 and 4, is focused in order to confine the sample to the downstream region (Figure 7a). When the sample has filled the intersection between the injection channels (i.e., 1 and 2) and the separation channels (i.e., 3 and 4), the electric field switches immediately to the dispensing step, and the sample plug is led into the separation channel, 6. Meanwhile, the sample in channels 1 and 2 and the buffer liquid in the channels 3 and 4 are kept motionless in order to prevent sample leakage (Figure 7b). The sample plug volume in the separation channel is notably smaller than in the two previous cases. Its size is determined to be approximately 0.46 and 0.483 times the size of the plug generated with a focusing ratio of $F/\phi = 1$ by the experimental method and the numerical model, respectively.

Figure 8 compares the sample shapes at the cross intersection of the single-cross configuration and the proposed double-cross

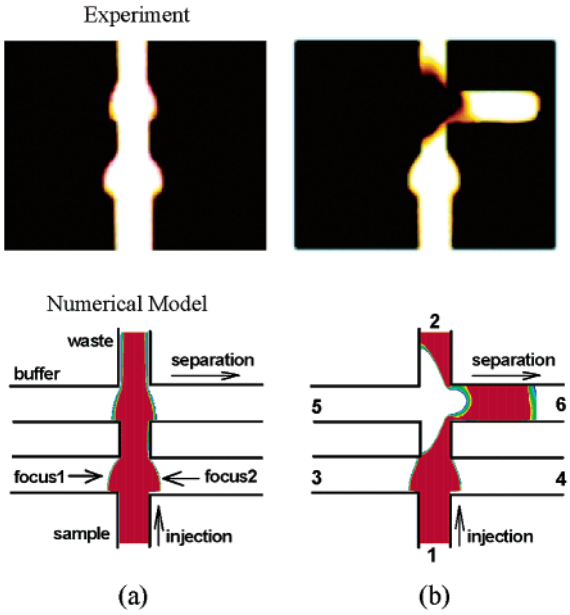

Figure 5. Sample distributions plot of the double-cross injection system for (a) loading steps and (b) dispensing steps for a focusing ratio $F/\phi = 1$.

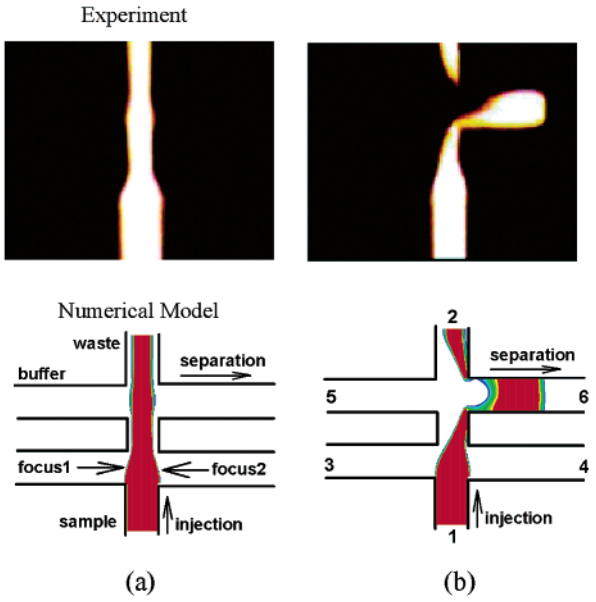

Figure 6. Sample distributions plot of the double-cross injection system for (a) loading steps and (b) dispensing steps for a focusing ratio $F/\phi = 1.4$.

injection system for different focusing ratios in the loading step. The sample plug is achieved by spatially confining it within the cross intersection before dispensing it into the separation channel. It is observed that the shape of the sample plug in the single-cross injection system is distorted, thus degrading the separation detection performance. However, in the case of the double-cross injection system, the valve is able to generate well-defined, short axial extent, and higher fluorescence signal[33] sample plugs, which are entirely suitable for high-performance separation.

Figure 9 presents electropherograms generated from images collected at the detection area of the single-cross and the double-cross injection systems for a focusing ratio of 1.4. The sample consists of 10^{-4} M Rhodamine B and 6.5×10^{-3} M Cy3 fluorescent dyes. The sample separation exhibits four obvious peaks, which correspond to the three fragments of Cy3 in the hydrolysate and the single fragment of Rhodamine B within the sample. The results presented in Figure 9a confirm the superior separation and detection ability of the proposed double-cross configuration microfluidic device.

Figure 10 presents the average volume of the sample plugs generated for different focusing ratios by the experimental method and the numerical model. It is noted that the maximum sample volume is generated when a focusing ratio of $F/\phi = 1$ is adopted. The average volume of the sample plugs was obtained by measuring 5 times during the experiment. The variation of the measurement was within 5%. For comparison purposes, the volume of the sample plug at this particular value of the focusing ratio is defined to be 1. A linear relationship is seen to exist between the volume of the sample plug (V) and the focusing ratio. Analysis shows this relationship to be given by $V \approx 1.689 - 0.675F/\phi$. This simple relationship is helpful in determining appropriate design parameters.

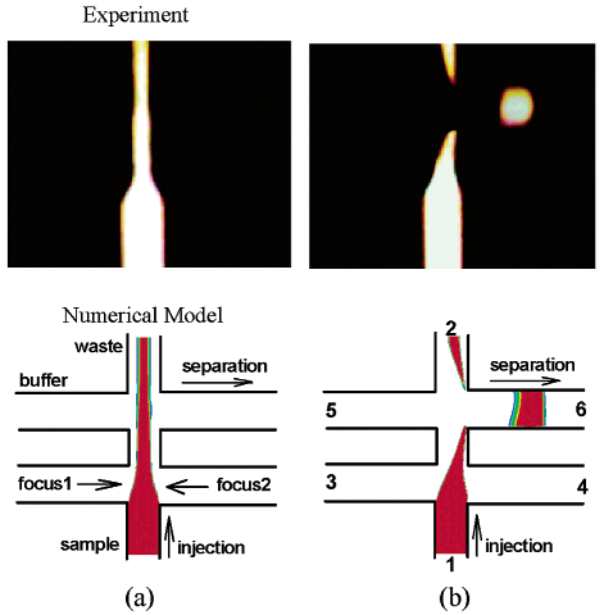

Figure 7. Sample distributions plot of the double-cross injection system for (a) loading steps and (b) dispensing steps for a focusing ratio $F/\phi = 1.8$.

CONCLUSIONS

This paper has presented an experimental and numerical investigation of two different injection systems on microfluidic chips, i.e., the single-cross form configuration and the proposed novel double-cross configuration design. Computer simulation has been shown to be a useful tool in representing the injection process of a sample into a separation channel. The current study demonstrates that the loading and dispensing steps of an injected sample plug may be controlled by the appropriate application of an electric potential. Further, it has been noted that the sample plug distribution produced by the single-cross injection system is inappropriate for electrophoresis separation purposes. A double-

(33) Jacobson, S. C.; Ramsey, J. M. *Anal. Chem.* **1997**, *69*, 3212−3217.

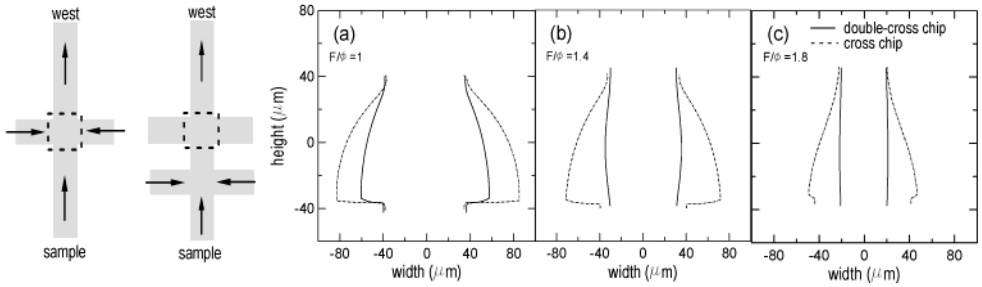

Figure 8. Comparison of the sample shapes at the cross intersection for different focusing ratios, i.e., (a) $F/\phi = 1$, (b) $F/\phi = 1.4$, and (c) $F/\phi = 1.8$ in the loading step for the cross injection system (dashed line) and the double-cross (solid line) injection system.

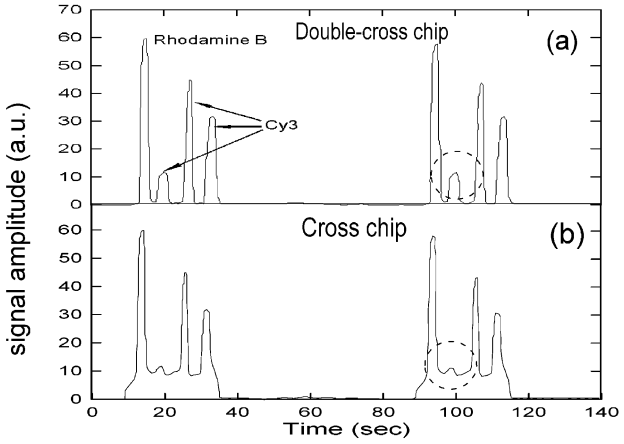

Figure 9. Electropherograms generated from an image collected at the detection area of the cross and double-cross injection systems for a focusing ratio $F/\phi = 1.4$.

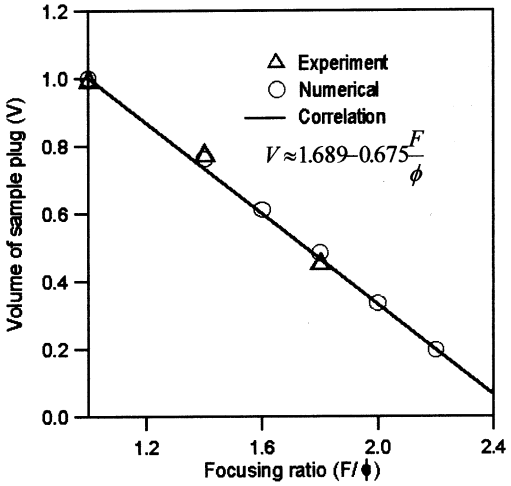

Figure 10. Comparison of the sample plug volume for various focusing ratios.

cross injection system, which combines the single-cross injection systems and the electrokinetic focusing technique on a single microfluidic chip, has been designed and its performance analyzed. Through the appropriate specification of the electric focusing ratio (F/ϕ), it has been shown that the proposed system is not only capable of performing the same function as the single-cross injection system but that it is also able to generate sample plugs of different volumes. Finally, the results indicate that the proposed design improves the sample plug distribution in the separation channel and thus results in a superior separation detection performance.

Received for review December 6, 2002. Accepted January 26, 2003.

AC020741D